Structural Eng./Earthquake Eng., JSCE, Vol. 13, No. 2, 137s—147s, 1996 October

SIMULATION OF SPACE-TIME VARIATION OF EARTHQUAKE GROUND MOTION USING A RECORDED TIME HISTORY

Hideji KAWAKAMI[1] and Makio ONO[2]

[1]Member of JSCE, Dr. of Eng., Professor, Dept. of Civil Eng., Saitama Univ. (Urawa 338, Japan)
[2]Member of JSCE, Tokyo Gas Corp.

Records of strong motion are often used as the ground motion inputs in earthquake response analysis and in the design of structures. The design of underground structures, however, requires more than just the time history at any particular point on the earth's surface. It also requires the space-time variation of the ground motion. We have therefore developed a method for generating a space-time variation that includes a strong ground motion recorded at a observation point. This simulated variation is characterized by an apparent velocity and by a coherence function. Here we presented a case study using motion recorded during the 1940 Imperial Valley earthquake.

Key Words : *earthquake, ground motion, simulation, underground structures*

1. INTRODUCTION

In the dynamic analysis and design of long underground structures such as tunnels, pipelines and buried pipes, the structure, soil and basement rock should be modeled and the seismic input motion should be determined at the soil or basement rock level as shown in **Fig.1**. Engineers are required to give input seismic motions at several points along the underground structure because the structural response is greatly affected by relative ground motion.

From this point of view, estimating simultaneous motion is an important problem to be solved, and techniques to simulate the space-time variation should be developed. In previous structural designs, records obtained from the one site near epicenters caused by earthquakes, such as the Imperial Valley, Taft, Tokachi-oki and Niigata earthquakes, have been used. Further, one of the following has frequently been assumed in establishing relative motion and in estimating space-time variation.

(1) One previously observed time history propagating horizontally with a finite constant propagating speed without distortion of wave form.

(2) Waves propagating horizontally with an infinite speed. Therefore, input motions are the same at all locations including their arrival times.

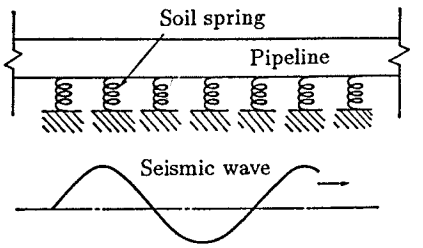

Fig.1 Physical model of underground pipelines (after Kubo[1])

Even when (1) is assumed, a problem still exists as to what value should be used for horizontal wave speed. This value differs greatly depending on whether the shear wave velocity of the surface layer is used as indicated by the standards[2] for gas pipelines in Japan or whether the value estimated from calculated cross-correlation functions using array records is used. For example, at alluvial sites, shear wave velocities are several hundred m/s, while the latter is several thousand m/s[3)~5)]. Using conventional theory[6] strain on the pipeline can be approximately estimated by

$$\text{(Strain on pipeline)} = \text{(Particle velocity of soil)} / \text{(Horizontal wave speed)} \quad (1)$$

It can be understood that these two kinds of

This paper is translated into English from the Japanese paper, which originally appeared on J. Struct. Mech. Earthquake Eng., JSCE, No.441/I-18, pp.167-175, 1992.1.

wave speeds will give us strains which differ as much as ten times. Even though the latter speed seems more rational, because distortion in the wave form has been neglected, strain will consequently be underestimated[7].

Assumption (2) has mainly been applied to sites with greatly varying horizontal soil structures. However, at some sites where horizontal soil structures have been found to be uniform as a result of geophysical exploration, vertically incident seismic waves do not create strain on the ground surface. Consequently, assumption (2) is also unsafe in estimating such sites[7]. In addition, distortion in the wave form has been neglected in both assumptions (1) and (2). However, in recent studies based on an analysis of seismic array records[7] distortion in the wave form has been shown to have a considerable effect on ground strains[8),9].

Several methods have been proposed to solve the above-mentioned problems. Shinozuka *et al.*[10),11)], Naganuma *et al.*[12)], Hoshiya *et al.*[13),14)], Harada *et al.*[15)~17)] and Deodatis *et al.*[18)] developed simulation methods for space-time variations with cross-correlation functions and cross-spectra equal to assumed ones. These studies were based on the random process theory, and space-time variation is interpreted as a function of time lag, the distance between two points, frequency and wavenumber. Further, simulation was conducted by taking wave propagation and distortion into consideration.

However, space-time variations obtained by each of these methods have not directly taken observed records into account, and consequently are too unrealistic and unconvincing to be used in actual design. Therefore, these simulated waves have not often been used as input motions, and one observed record and assumption (1) or (2) are still frequently being used in practice.

Such a tendency is also true in the design of buildings, and observed actual records, such as those from Imperial Valley, Taft and Tokachi-oki, have often been used as input seismic motions rather than simulated time histories based on random process theory. This tendancy is due to the idea that the observed must be more realistic than the simulated. Furthermore, in the design of underground structures, not only observed time history records but also space-time variations around the structure are required, because relative motion is the main cause behind strain induced in the structure. Because of reasons such as these, one seismic record is insufficient in designing, and space-time variations are still required. In particular, several representative space-time variations including well-known observed records are believed to be essential when designing underground structures such as in building extensions.

The authors have already proposed a method using a double Fourier series for the rational simulation of space-time variations considering the distortion of wave forms during propagation[19)]. The objective of this paper is to develop another method extending the theory of multiply-correlated random processes instead of the double Fourier series and to demonstrate the effectiveness of the proposed method.

In this paper, space-time variation is represented by multiply-correlated random processes $U_i(t)$ in which i and t denote location and time, respectively. Also, similar to our previous papers[19),20)], the following conditions have been assumed for simulated space-time variation.

Condition A: Auto-correlation functions of both simulated space-time variation and observed record should be identical. Based on the auto-correlation function of the observed record, wave propagation speed and the degree of wave distortion, cross-correlation functions or cross-spectra have been assumed. Cross-correlation functions of simulated space-time variations should also be identical with assumed ones.

Condition B: Simulated space-time variations should include the observed record.

In this paper, regarding condition A, cross-correlation functions have been assumed to represent wave propagation in the positive direction and a decrease in correlation with increasing distance between two points. Concerning condition B, space-time variation whose component $U_1(t)$ matches the observed record has been simulated. A case study is presented using the El Centro record during the Imperial Valley earthquake, satisfying the above two conditions.

2. THEORY

(1) Simulation of space-time variation with continuous cross-spectra

Space-time variation of earthquake ground displacement is expressed by m cross-correlated stochastic processes $U_i(t)$ $(i=1,...,m)$, where i and t denote location and time, respectively. The formulation presented in this paper is applicable not only to displacements but also to velocities and accelerations.

Shinozuka *et al.*[21)] and Hoshiya[22)] have shown that stochastic processes $U_i(t)$ $(i=1,...,m)$ can be expressed by using one-sided continuous cross-spectra $S_{XT}(x_0,\omega)$, where ω and x_0 respectively denote the angular frequency and distance be-

tween two points, as follows.

$$U_i(t) = \sum_{p=1}^{i} \sum_{n=1}^{N} |H_{ip}(\omega_n)|\sqrt{2\Delta\omega} \cdot \cos\{\omega_n t + \theta_{ip}(n) + \phi_{pn}\} \quad (i=1,2,\cdots,m) \quad (2)$$

where ϕ_{pn} are mutually independent and uniformly distributed random variables from zero to 2π, ω_n is the nth discretized angular frequency,

$$\omega_n = n \cdot \Delta\omega = \frac{2n\pi}{T} \qquad (n=1,2,\cdots,N) \quad (3)$$

and T is the duration of the record. In this paper, the constant component has been neglected, and the stationarity of the random process has been assumed over the period from 0 to T.

Term $H_{ip}(\omega)$ can be obtained by factoring the matrix as follows.

$$\begin{bmatrix} S_{11}(\omega) & \cdots & S_{1m}(\omega) \\ \vdots & \ddots & \vdots \\ S_{m1}(\omega) & \cdots & S_{mm}(\omega) \end{bmatrix} = \begin{bmatrix} H_{11}^*(\omega) & & 0 \\ \vdots & \ddots & \\ H_{m1}^*(\omega) & \cdots & H_{mm}^*(\omega) \end{bmatrix} \cdot \begin{bmatrix} H_{11}(\omega) & \cdots & H_{m1}(\omega) \\ & \ddots & \vdots \\ 0 & & H_{mm}(\omega) \end{bmatrix} \quad (4)$$

where $*$ indicates the complex conjugate, and

$$S_{ij}(\omega) = S_{XT}(x_0|_{ij}, \omega) \quad (5)$$

where $x_0|_{ij}=x_i - x_j$ is the relative distance between two points i and j. Further, term $\theta_{ip}(n)$ in Eq.(2) is given by

$$\theta_{ip}(n) = \tan^{-1}\left(\frac{I_m[H_{ip}(\omega_n)]}{R_e[H_{ip}(\omega_n)]}\right) \quad (6)$$

where R_e and I_m indicate real and imaginary parts, respectively.

(2) Simulation of space-time variation with line cross-spectra

To discretize Eq.(2), $H_{ip}(\omega_n)\sqrt{\Delta\omega}$ has been considered as a group, and Eq.(2) has been rewritten as

$$U_i(t) = \sum_{p=1}^{i} \sum_{n=1}^{N} |H_{ip}(\omega_n)\sqrt{\Delta\omega}|\sqrt{2} \cdot \cos\{\omega_n t + \theta_{ip}(n) + \phi_{pn}\} \quad (i=1,2,\cdots,m) \quad (7)$$

where $H_{ip}(\omega)\sqrt{\Delta\omega}$ can be obtained by factoring the line cross-spectral matrix

$$\begin{bmatrix} S_{11}(\omega)\Delta\omega & \cdots & S_{1m}(\omega)\Delta\omega \\ \vdots & \ddots & \vdots \\ S_{m1}(\omega)\Delta\omega & \cdots & S_{mm}(\omega)\Delta\omega \end{bmatrix} = \begin{bmatrix} H_{11}^*(\omega)\sqrt{\Delta\omega} & & 0 \\ \vdots & \ddots & \\ H_{m1}^*(\omega)\sqrt{\Delta\omega} & \cdots & H_{mm}^*(\omega)\sqrt{\Delta\omega} \end{bmatrix} \begin{bmatrix} H_{11}(\omega)\sqrt{\Delta\omega} & \cdots & H_{m1}(\omega)\sqrt{\Delta\omega} \\ & \ddots & \vdots \\ 0 & & H_{mm}(\omega)\sqrt{\Delta\omega} \end{bmatrix} \quad (8)$$

where

$$S_{ij}(\omega)\Delta\omega = S_{XT}(x_0|_{ij}, \omega)\Delta\omega \quad (9)$$

Phase $\theta_{ip}(n)$ can also be given by

$$\theta_{ip}(n) = \tan^{-1}\left(\frac{I_m[H_{ip}(\omega_n)\sqrt{\Delta\omega}]}{R_e[H_{ip}(\omega_n)\sqrt{\Delta\omega}]}\right) \quad (10)$$

and ϕ_{pn} represent mutually independent and uniformly distributed random variables from zero to 2π.

(3) Power spectrum of observed record

As mentioned in condition A in **1**, simulated space-time variation should have the same power spectrum as the observed record. The Fourier series expansion of the observed record is given as

$$F(t) = \sum_{n=1}^{N} \{a_n \cos(\omega_n t) + b_n \sin(\omega_n t)\} \quad (11)$$

From Eq.(11), ground motion at time $t+\tau$ can be expressed as

$$F(t+\tau) = \sum_{n=1}^{N} [\, a_n \cos\{\omega_n(t+\tau)\} + b_n \sin\{\omega_n(t+\tau)\}\,] \quad (12)$$

where τ is time lag. By considering the product of $F(t)$ and $F(t+\tau)$ and taking the temporal average from 0 to T, auto-correlation function $R_{XT}(0,\tau)$ is obtained as

$$R_{XT}(0,\tau) = \overline{F(t)\cdot F(t+\tau)} = \frac{1}{2}\sum_{n=1}^{N}(a_n^2 + b_n^2)\cos(\omega_n\tau) \quad (13)$$

where $\overline{\quad}$ indicates the temporal average. The Fourier transform of Eq.(13) yields the two-sided power spectrum

$$\frac{1}{2\pi}\int_{-\infty}^{\infty} R_{XT}(0,\tau)\exp(-i\,\omega\tau)\,d\tau = \frac{1}{4}\sum_{n=1}^{N}(a_n^2 + b_n^2)\{\delta(\omega-\omega_n) + \delta(\omega+\omega_n)\}$$

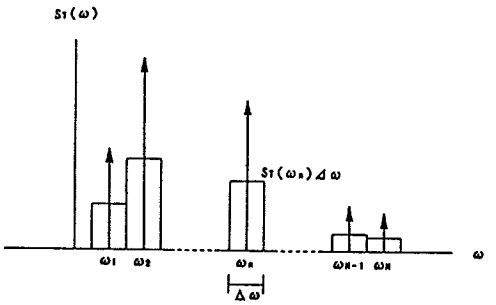

Fig.2 Line spectrum

(14)

where $\delta(\omega)$ denotes Dirac's delta function. Therefore, the one-sided power spectrum $S_T(\omega)$ can be given by

$$S_T(\omega) = \frac{1}{2}\sum_{n=1}^{N}(a_n^2 + b_n^2)\,\delta(\omega-\omega_n) \qquad (15)$$

and is indicated by the arrows in **Fig.2**. By integrating Eq.(15) from $\omega_n - \Delta\omega/2$ to $\omega_n + \Delta\omega/2$, a relationship can be established between the one-sided power spectrum and Fourier coefficients.

$$S_T(\omega_n)\,\Delta\omega = \frac{(a_n^2 + b_n^2)}{2} \qquad (16)$$

(4) Assumptions of cross-spectra

Simulated space-time variation should have an identical power spectrum to that of the observed record as mentioned in condition A, and the correlation between two simulating points should decrease with wave propagation. From previous studies[23)–25)] on comparisons between two actually observed time histories, correlation is known to decrease with increasing distance between observation points, $|x_0|$, and with increasing frequencies.

Hence, one-sided cross-spectrum $S_{XT}(x_0,\omega)$ is assumed as

$$S_{XT}(x_0,\omega) = S_T(\omega)\,\exp(-i\,\omega x_0/c)A(|\omega||x_0|/c) \qquad (17)$$

where $A()$ is a function of frequency $|\omega|$ and travel time $|x_0|/c$. Further, c and $S_T(\omega)$ are the horizontal speed of the propagating wave and the observed one-sided power spectrum, respectively. Function $A()$ is called coherency, and by referring to a previous study[23)], it can be assumed to be written as

$$A(|\omega||x_0|/c) = \exp\{-\alpha|\omega||x_0|/(2\pi c)\} \qquad (18)$$

where α denotes the degree of distortion of time history due to propagation, or the distortion coefficient[7),19),20)]. By definition, a zero value for α is free of distortion, whereas a large value for α greatly decreases the correlation between the two time histories.

(5) Cross-spectrum of space-time variation

Multiplying both sides of Eq.(17) by $\Delta\omega$, the relationship between line cross- and power spectra can be given by

$$S_{XT}(x_0\,,\omega_n)\,\Delta\omega = S_T(\omega_n)\,\Delta\omega \cdot \exp\{-\alpha|\omega_n||x_0|/(2\pi c)\}\exp(-i\,\omega_n x_0/c) \qquad (19)$$

Then, substituting Eq.(16) into Eq.(19), the cross-spectrum of space-time variation yields

$$S_{XT}(x_0,\omega_n)\,\Delta\omega = \frac{(a_n^2 + b_n^2)}{2} \cdot \exp\{-\alpha\,|\omega_n||x_0|/(2\pi c)\}\exp(-i\,\omega_n x_0/c) \qquad (20)$$

An assumed corresponding cross-correlation function can also be obtained by the inverse Fourier transformation of the two-sided cross-spectrum.

$$R_{XT}^0(x_0,\tau) = \frac{1}{2}\int_{-\infty}^{\infty} S_{XT}(x_0,\omega)\exp(i\,\omega\tau)\,d\omega = \frac{1}{2}\sum_{n=1}^{N}(a_n^2 + b_n^2)\exp\{-\alpha|\omega_n||x_0|/(2\pi c)\} \cdot \cos\{\omega_n(\tau - x_0/c)\} \qquad (21)$$

(6) Space-time variation including observed record

Regarding condition B, first process $U_1(t)$ has been chosen from m processes $U_i(t)$ (i=1, ..., m) in Eq.(7),

$$U_1(t) = \sum_{n=1}^{N} |\,H_{11}(\omega_n)\sqrt{\Delta\omega}|\sqrt{2} \cdot \cos\{\omega_n t + \theta_{11}(n) + \phi_{1n}\} \qquad (22)$$

and it has been matched with the observed record.

In the above equation, terms $|H_{11}(\omega_n)\sqrt{\Delta\omega}|$ and $\theta_{11}(n)$ can be estimated as follows. From Eqs.(9) and (8),

$$S_{11}(\omega_n)\,\Delta\omega = H_{11}^*(\omega_n)\,\sqrt{\Delta\omega}\cdot H_{11}(\omega_n)\,\sqrt{\Delta\omega} \qquad (23)$$

$$S_{11}(\omega_n)\,\Delta\omega = S_{XT}(0,\omega_n)\,\Delta\omega = S_T(\omega_n)\,\Delta\omega \qquad (24)$$

Substituting Eq.(16) into Eqs.(23) and (24) and ensuring that $S_T(\omega_n)\Delta\omega$ is not a negative value, we derive

$$R_e[H_{11}(\omega_n)\,\sqrt{\Delta\omega}] = \sqrt{(a_n^2 + b_n^2)/2} \qquad (25)$$

$$I_m[H_{11}(\omega_n)\,\sqrt{\Delta\omega}] = 0 \qquad (26)$$

Therefore,

$$|H_{11}(\omega_n)\sqrt{\Delta\omega}| = \sqrt{(a_n^2+b_n^2)/2} \quad (27)$$

$$\theta_{11}(n) = 0 \quad (28)$$

Finally, time history $U_1(t)$ yields

$$U_1(t) = \sum_{n=1}^{N} \sqrt{a_n^2+b_n^2}\cos(\omega_n t + \phi_{1n}) \quad (29)$$

However, the Fourier series of the observed record given by Eq.(11) can be rewritten as

$$F(t) = \sum_{n=1}^{N} A_n \cos(\omega_n t + \beta_n) \quad (30)$$

where

$$A_n = \sqrt{a_n^2+b_n^2} \quad (31)$$

$$\beta_n = \tan^{-1}(-b_n/a_n) \quad (32)$$

From a comparison between Eqs.(29) and (30), ϕ_{1n} in Eq.(22) can be established as

$$\phi_{1n} = \beta_n = \tan^{-1}(-b_n/a_n) \quad (33)$$

After all, if ϕ_{1n} in Eq.(33) is used, simulated time history $U_1(t)$ in Eq.(2) is the same as the observed one.

In previous studies on methods for unconditional simulations of space-time variation, all values of ϕ_{in} (i=1, ..., m, n=1, ..., N) have been simulated as mutually independent and uniformly distributed random variables. However, in this study, ϕ_{1n} (n=1, ..., N) have been determined by Eq.(33) to satisfy condition B, and remaining members ϕ_{in} (i=2, ..., m, n=1, ..., N) have been simulated as mutually independent and uniformly distributed random variables.

(7) Summary of algorithm of developed method

The developed simulation method for space-time variation including the one observed record can be summarized as follows:

i) Calculate Fourier coefficients, a_n and b_n, by expanding the observed record into a Fourier series as shown by Eq.(11).

ii) Choose site location x_i where the time history should be simulated as the ith random process.

iii) Assume a cross-spectrum by using Eq.(20), after estimating horizontal speed of propagating wave c and distortion coefficient α.

iv) Factor the cross-spectral matrix into two triangular matrices as shown by Eq.(8), and estimate $|H_{ip}(\omega_n)\sqrt{\Delta\omega}|$ and $\theta_{ip}(n)$.

v) Calculate ϕ_{1n} (n=1, ..., N) by using Eq.(33).

vi) Generate mutually independent and uniformly distributed random variables for values of ϕ_{in} (i=2, ..., m, n=1, ..., N).

vii) Calculate space-time variation by using Eq.(7).

(8) Error in cross-correlation function of simulated random process

In the above theory, a method has been developed to simulate space-time variations whose cross-spectrum and cross-correlation function are "identical" with assumed ones based on observed time history. However, as the meaning of the word "identical" is not particularly clear, it will be examined in this section.

Cross-correlation function between simulated random processes at two separated points with distance x_0 can be given by

$$R_{XT}(x_0|_{ij},\tau) = \overline{U_i(t)\cdot U_j(t+\tau)}$$
$$= \sum_{p=1}^{i}\sum_{q=1}^{j}\sum_{n=1}^{N} |H_{ip}(\omega_n)\sqrt{\Delta\omega}||H_{jq}(\omega_n)\sqrt{\Delta\omega}|$$
$$\cdot\cos[\omega_n\tau - \{\theta_{ip}(n)-\theta_{jq}(n)\} - (\phi_{pn}-\phi_{qn})] \quad (34)$$

In the above equation, the cross-correlation function depends on values ϕ_{1n} and also on random variables, ϕ_{pn} and ϕ_{qn} (p,q=2, ..., m, n=1, ..., N), except when i=j=1. The cross-correlation functions of simulated space-time variation obviously depend on samples, and these are not exactly equal to assumed ones. This is also true for auto-correlation functions $R_{XT}(0,\tau)$, where i=$j\neq$1.

However, when an ensemble average is taken with respect to random variables ϕ_{pn} and ϕ_{qn} (p,q=2, ..., m, n=1, ..., N), all terms except p=q vanish in Eq.(34). When this occurs,

$$E\left[R_{XT}(x_0|_{ij},\tau)\right] = \sum_{p=1}^{\mathrm{Min}(i,j)}\sum_{n=1}^{N} |H_{ip}(\omega_n)\sqrt{\Delta\omega}|$$
$$\cdot|H_{jp}(\omega_n)\sqrt{\Delta\omega}|\cos[\omega_n\tau - \{\theta_{ip}(n)-\theta_{jp}(n)\}] \quad (35)$$

where $\mathrm{Min}(i,j)$ indicates the smaller value of the two numbers i and j. Considering the following relationship,

$$S_{ij}(-\omega) = S_{ij}^*(\omega) \quad (36)$$

the following equations are derived[21].

$$H_{ip}(-\omega)\sqrt{\Delta\omega} = H_{ip}^*(\omega)\sqrt{\Delta\omega} \quad (37)$$

$$\theta_{ip}(-n) = -\theta_{ip}(n) \quad (38)$$

Consequently, the ensemble average of simulated cross-correlation functions in Eq.(35) is identical

with the assumed one as shown by

$$
\begin{aligned}
&E\left[R_{XT}(x_0|_{ij},\tau)\right] \\
&= \frac{1}{2}\sum_{p=1}^{\mathrm{Min}(i,j)}\sum_{n=1}^{N}\Big[|H_{ip}(\omega_n)\sqrt{\Delta\omega}||H_{jp}(\omega_n)\sqrt{\Delta\omega}| \\
&\qquad \cdot\cos[\omega_n\tau-\{\theta_{ip}(n)-\theta_{jp}(n)\}] \\
&\quad +|H_{ip}(-\omega_n)\sqrt{\Delta\omega}||H_{jp}(-\omega_n)\sqrt{\Delta\omega}| \\
&\qquad \cdot\cos[-\omega_n\tau-\{\theta_{ip}(-n)-\theta_{jp}(-n)\}]\Big] \\
&= \frac{1}{2}\sum_{p=1}^{\mathrm{Min}(i,j)}\sum_{n=-N}^{N}|H_{ip}(\omega_n)\sqrt{\Delta\omega}||H_{jp}(\omega_n)\sqrt{\Delta\omega}| \\
&\qquad \cdot\cos[\omega_n\tau-\{\theta_{ip}(n)-\theta_{jp}(n)\}] \\
&= \frac{1}{2}\sum_{p=1}^{\mathrm{Min}(i,j)}\sum_{n=-N}^{N}|H_{ip}(\omega_n)\sqrt{\Delta\omega}||H_{jp}(\omega_n)\sqrt{\Delta\omega}| \\
&\qquad \cdot\exp[i\{\omega_n\tau-\theta_{ip}(n)+\theta_{jp}(n)\}] \\
&\qquad (\because \text{Imaginary part is a odd function with respect to } \omega) \\
&= \frac{1}{2}\sum_{p=1}^{\mathrm{Min}(i,j)}\sum_{n=-N}^{N}H^*_{ip}(\omega_n)\sqrt{\Delta\omega}\cdot H_{jp}(\omega_n)\sqrt{\Delta\omega} \\
&\qquad \cdot\exp(i\,\omega_n\tau) \\
&= \frac{1}{2}\sum_{n=-N}^{N}S_{ij}(\omega_n)\,\Delta\omega\cdot\exp(i\,\omega_n\tau) \\
&\simeq \frac{1}{2}\int_{-\infty}^{\infty}S_{ij}(\omega)\cdot\exp(i\,\omega\tau)\,d\omega \\
&= R^0_{XT}(x_0|_{ij},\tau) \qquad (39)
\end{aligned}
$$

In this study, although ϕ_{1n} (n=1, ..., N) are not random variables, the above results hold true even when ϕ_{1n} are random variables[21].

From the above discussion, it should be noted that using the random process theory, which includes the proposed method, it is not possible to simulate a sample for the space-time variation where the cross-correlation function is exactly identical with the assumed one. This means that simulated space-time variation involves some errors which have been expressed by the terms $p\neq q$ in Eq.(34). However, these terms vanish when an ensemble average is taken, and the ensemble average of the simulated cross-correlation functions shown in Eq.(39) is identical with the assumed one.

3. SIMULATION USING IMPERIAL VALLEY EARTHQUAKE RECORD

In this section, numerical results are presented using records taken from the El Centro site during the Imperial Valley earthquake (May 18, 1940).

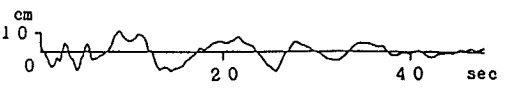

Fig.3 Observed wave during Imperial Valley earthquake (1940)[27]

These records are frequently used for the dynamic analysis of structures. The maximum acceleration of the NS component is 341.7 cm/s^2. The displacement time history estimated from the numerical integration of the acceleration record has also been open to the public as shown by **Fig.3**[27], and the maximum value of displacement is 10.9 cm. During simulation, the first 48 sec of the record was used, and the first to the 29th Fourier coefficients were calculated.

Several cases as shown by **Table 1** were analyzed. In Case 1, wave horizontally propagating speed c and distortion coefficient α have respectively been assumed as 1,000 m/s and $0.2\times 2\pi$. The value of the distortion coefficient was determined based on Ishii's study[23]. Here, the corresponding cross-correlation function given by Eq.(21) has been assumed as shown by **Fig.4**. The thick line at x_0=0 in **Fig.4** indicates the auto-correlation function of observed time history.

Time histories have been simulated at 31 points that are distributed over -6 to $+6$ km with an equal distance between adjacent points of 0.4 km. Among time histories $U_i(t)$ (i=1, ..., 31), subscript i=1 in $U_i(t)$ denotes the recording point at x=0, and even and odd numbers of i ($2\leq i\leq 31$) denote simulating points located at positive and negative sides of x=0, respectively. The distance between the simulating point and recording point x=0 increases with increasing subscript i.

Fig.5 shows space-time variation simulated by following the algorithm summarized in **2(7)**. It should be noted that the simulated time history at point i=1 (x=0) indicated by the thick line in **Fig.5** is completely identical with the observed record shown in **Fig.3**, therefore satisfying Condition B. **Fig.6** shows cross-correlation functions, in the space and time domain of $-24<\tau<+24$sec and $-6<x_0<+6$km, calculated from the simulated space-time variation sample in **Fig.5**.

Fig.7 shows space-time variation obtained in a similar manner to **Fig.5** but by using another set of random variables for ϕ_{pn}. Cross-correlation functions of the variation in **Fig.7** are also shown in **Fig.8**.

In **Figs.6 and 8**, it should be noticed that the simulated cross-correlation function of each sam-

Table 1 Used parameters and figure numbers in Cases 1 to 5

	Propagation speed c(m/s)	Distortion coefficient α	Assumed cross-correlation	Simulated space-time variation	Cross-correlation of one sample	Ensemble average of 100 samples
Case 1	1000	$0.2\times2\pi$	**Fig. 4**	**Figs.5 and 7**	**Figs.6 and 8**	**Fig. 9**
Case 2	2000	$0.2\times2\pi$	**Fig.10**	**Fig.11**		**Fig.12**
Case 3	500	$0.2\times2\pi$	**Fig.13**	**Fig.14**		**Fig.15**
Case 4	1000	$0.1\times2\pi$	**Fig.16**	**Fig.17**		**Fig.18**
Case 5	1000	$0.4\times2\pi$	**Fig.19**	**Fig.20**		**Fig.21**

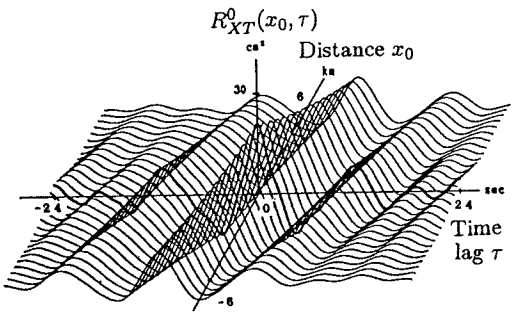

Fig.4 Assumed cross-correlation function (Case 1)

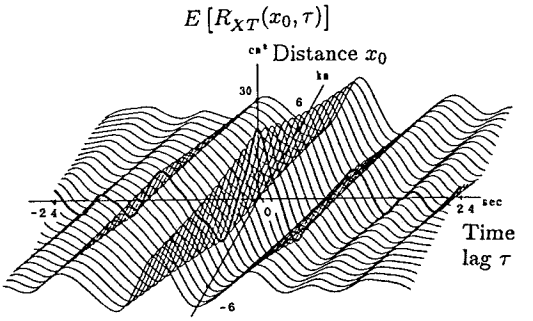

Fig.9 Ensemble average of cross-correlation function from 100 samples (Case 1)

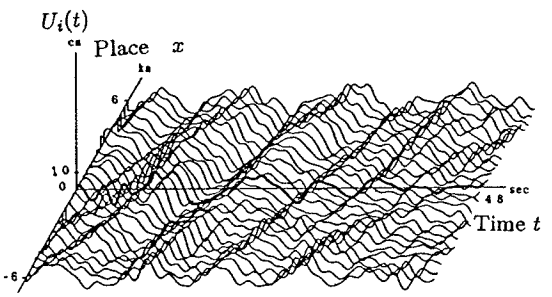

Fig.5 Simulated space-time variation (Case 1)

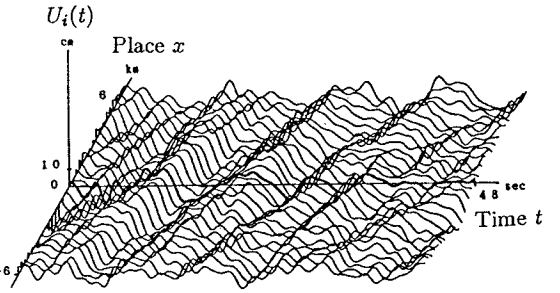

Fig.7 Another sample of simulated space-time variation (Case 1)

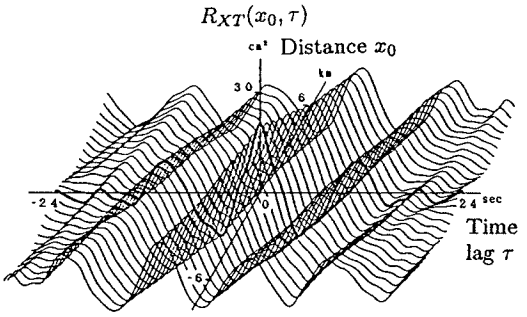

Fig.6 Cross-correlation function of variation sample in **Fig.5** (Case 1)

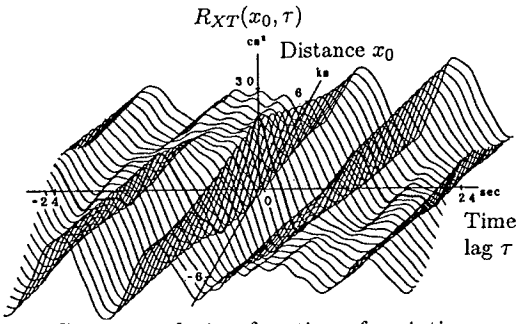

Fig.8 Cross-correlation function of variation sample in **Fig.7** (Case 1)

ple is nearly, but not exactly, equal to the assumed one shown in **Fig.4**. However, as shown in **2(8)**, their ensemble average should be identical with the assumed cross-correlation function. To verify this, simulations were conducted one hundred times and the ensemble average was calculated. The results are shown in **Fig.9**, and it can be noticed that they are identical to those in **Fig.4**.

For the other cases (Cases 2 to 5) summarized in **Table 1**, space-time variations have also been calculated using different sets of horizontally

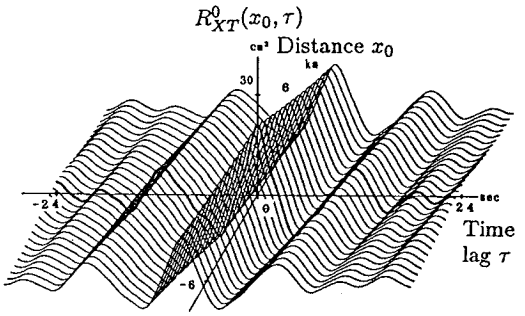

Fig.10 Assumed cross-correlation function (Case 2)

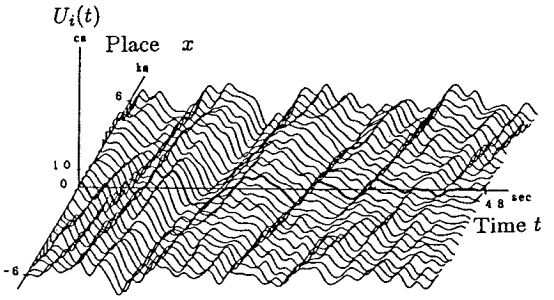

Fig.11 Simulated space-time variation (Case 2)

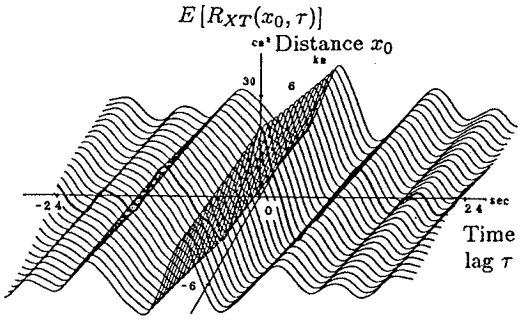

Fig.12 Ensemble average of cross-correlation function from 100 samples (Case 2)

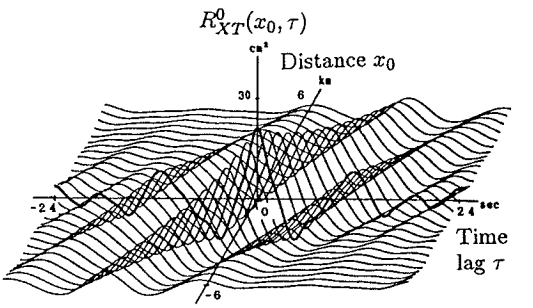

Fig.13 Assumed cross-correlation function (Case 3)

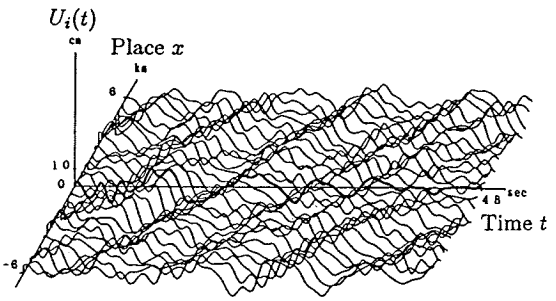

Fig.14 Simulated space-time variation (Case 3)

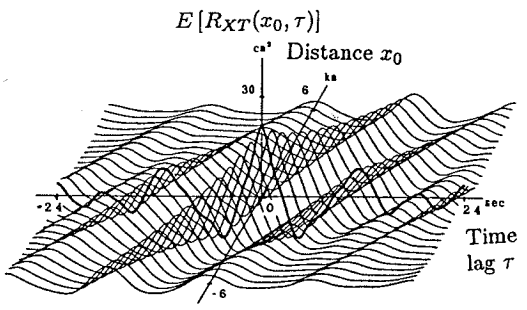

Fig.15 Ensemble average of cross-correlation function from 100 samples (Case 3)

propagating wave speed c and distortion coefficient α. For each of these cases, assumed cross-correlation function, simulated sample of space-time variation, and ensemble average of cross-correlation functions of one-hundred simulated samples are shown in **Figs.10** to **21**, and the corresponding figure numbers are indicated in **Table 1**.

In Cases 1, 2 and 3, horizontally propagating wave speed c can be read from the velocity of the shift of peaks in **Figs.5** (or **7**), **11** and **14**. Meanwhile, comparisons between **Figs.5** (or **7**), **17** and **20** in Cases 1,4 and 5 show the effects of distortion coefficient α on the degree of distortion during wave propagation.

Similar to the previous comparison between **Figs.4** and **6**, the cross-correlation function of the simulated sample in Cases 2 to 5 is also nearly, but not exactly, equal to the assumed one. However, the ensemble average of one hundred samples of cross-correlation functions had a good agreement with the assumed one, and such results are shown in **Figs.10**, **12**, **13**, **15**, **16**, **18**, **19** and **21**. The above results mean that condition A is satisfied in all cases.

Regarding condition B, the simulated time histories at point x=0 indicated by the thick lines in **Figs.11**, **14**, **17** and **20** are identical with the observed record in **Fig.3**. Therefore, it can be confirmed that condition B is also satisfied.

In this section, several examples of the application of the method developed in the previous sec-

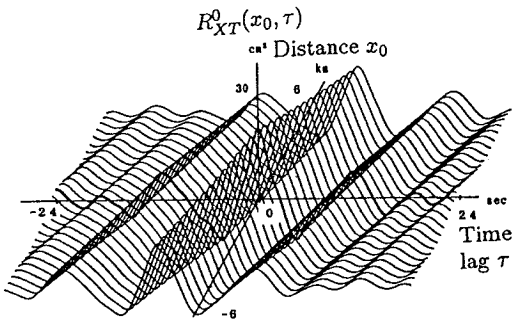

Fig.16 Assumed cross-correlation function (Case 4)

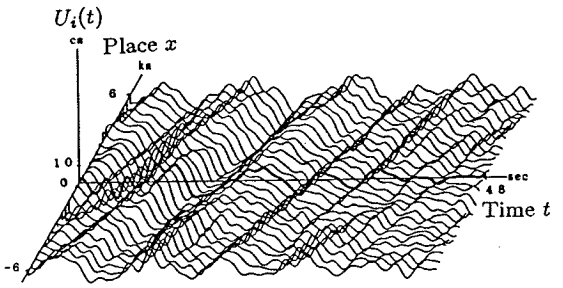

Fig.17 Simulated space-time variation (Case 4)

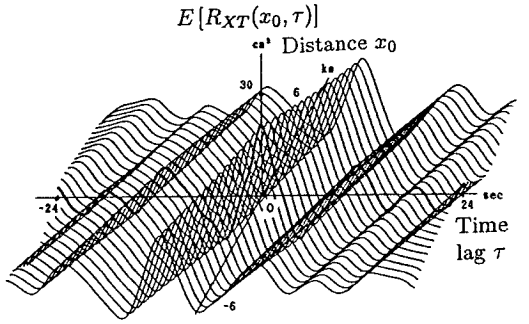

Fig.18 Ensemble average of cross-correlation function from 100 samples (Case 4)

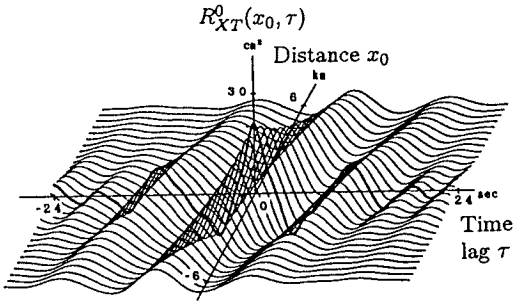

Fig.19 Assumed cross-correlation function (Case 5)

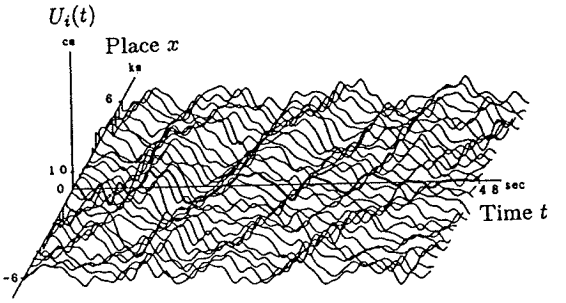

Fig.20 Simulated space-time variation (Case 5)

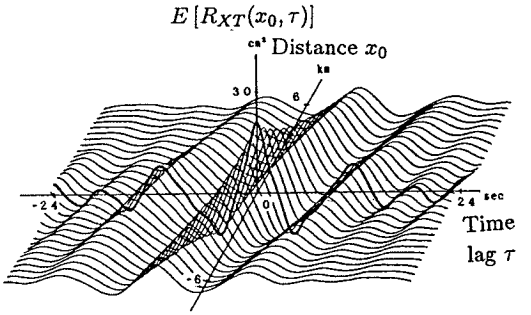

Fig.21 Ensemble average of cross-correlation function from 100 samples (Case 5)

tion have been demonstrated, and the effects of parameters used have been illustrated. However, the values of parameters are only based on a few previous studies. To utilize simulated space-time variation in the design of structures, the values of these parameters should be investigated in more detail by using a number of seismic array records observed under various ground conditions.

4. CONCLUSIONS

In designing underground structures to withstand earthquakes, the estimation of space-time variations around the structure is an important problem to be solved. The objective of this paper has been to simulate space-time variations that include observed records.

In this paper, the following two conditions have been considered.

Condition A is that the temporal auto-correlation functions (and power spectra) of both space-time variation and the observed record should be same. The cross-correlation function (or cross-spectrum) is assumed using the auto-correlation function of the observed record and the following two parameters, i.e., wave horizontally propagating speed c and distortion coefficient α related to coherency. The cross-correlation function of the simulated space-time variation should be identical with the assumed one.

Condition B is that simulated space-time variation should include the observed record.

The authors proposed a method using the double Fourier series in their previous papers[19),20)]. In this paper, a new method has been developed to simulate space-time variation based on the theory of multiply-correlated random processes. In the case study, the Imperial Valley earthquake record was used, and cross-correlation functions have been assumed so that seismic waves propagate in the positive direction and correlation decreases with wave propagation. Under these assumptions, space-time variation has been simulated and the following conclusions have been derived:

1) Simulated space-time variation includes the observed record;

2) The auto- or cross-correlation function of the simulated space-time variation sample is nearly equal to the assumed one; and

3) Ensemble average of the auto- or cross-correlation function of the simulated space-time variation samples is exactly equal to the assumed one.

Features 2 and 3 above are also true in the previous simulation methods of the multiply-correlated random processes, however, they are not true according to the method shown in the authors' previous papers[19),20)]. In other words, the method developed here has softened condition B, and this has made it much easier to find the solution by eliminating troublesome convergence calculations. Because of this, the proposed method is believed to be one of the simplest and most effective methods to simulate conditional space-time variations.

REFERENCES

1) Kubo K.: *Earthquakes and Civil Engineering Structures*, Kashima Press, Tokyo, p.127, 1981 (in Japanese).
2) Japanese Government: Notice on details of technical standards of facilities of oil pipelines, No.125, 1973 (in Japanese).
3) Tsuchida, H. and Kurata, E.: Observation of earthquake response of ground with horizontal and vertical seismometer arrays, *Proc. of the 4th Japan Earthquake Engineering Symposium*, pp.137-144, 1975.
4) Tsuchida, H. and Iai, S.: Observation of earthquake response of ground with horizontal and vertical seismometer arrays (2nd report), *Proc. of the 5th Japan Earthquake Engineering Symposium*, pp.169-176, 1980.
5) Tamura, T., Kato K. and Maeda, H.: Characteristics of earthquake ground motions along a line at alluvial sites, *29th Annual Meeting, JSCE*, 538-539, 1974 (in Japanese).
6) Sakurai, A.: Earthquake engineering for underground pipelines based on analysis of ground motions, Doctoral thesis, Waseda University, 1971 (in Japanese).
7) Kawakami, H. and Sato Y.: Effect of distortion of seismic waves on estimated value of ground relative displacement or strain. *Proc. JSCE*, No.337, pp.37-46, 1983 (in Japanese).
8) Katayama, T., Farjoodi, J. and Sato, N.: Measurement of seismic ground strain by a dense seismograph array, *Proc. 8th World Conference on Earthquake Engineering*, Vol.II, pp.207-214, 1984.
9) Takada, S. and Wright, J.P.: Earthquake relative motions for lifelines, *Proc. JSCE*, No.299, pp.13-21, 1980 (in Japanese).
10) Shinozuka, M. and Lenoe, E.: A probabilistic model for spatial distribution of material properties, *Engineering Fracture Mechanics*, Vol.8, pp.217-227, 1976.
11) Shinozuka, M., Kameda, H. and Koike, T.: Ground strain estimation for seismic risk analysis, *Journal of Engineering Mechanics*, ASCE, Vol. 109, No.1, pp.175-191, 1983.
12) Naganuma, T. Deodatis, G. and Shinozuka, M.: ARMA model for two-dimensional processes, *Journal of Engineering Mechanics*, ASCE, Vol.113, No.2, pp.234-251, 1987.
13) Hoshiya, M., Ishii, K. and Kurita, H.: Simulation of spatially and temporally variative earthquake ground motions, *Proc. JSCE*, No.386/I-8, pp.359-367, 1987 (in Japanese).
14) Hoshiya, M. and Chiba, T.: Simulation methods of multi-dimensional nonstationary stochastic processes by time domain models, *Proc. JSCE*, No.296, pp.121-130, 1980.
15) Harada, T. and Shinozuka, M.: Probabilistic response of surface layer and space-time power spectrum of earthquake motions, *19th Japan Earthquake Engineering Meeting*, pp.33-36, 1987 (in Japanese).
16) Inagasa T. and Harada, T.: Response of surface layer with probabilistic characteristics and space-time power spectrum of earthquake motions, *43th Annual Meeting, JSCE*, I-463, pp.976-977, 1988 (in Japanese).
17) Harada, T. and Shinozuka, M.: Stochastic analysis of seismic ground motions in space and time, *Proc. 9th World Conference on Earthquake Engineering*, pp.II-825-830, 1988.
18) Deodatis, G. and Shinozuka, M.: Digital simulation of seismic ground motion using stochastic wave theory, *Proc. 9th World Conference on Earthquake Engineering*, pp.II-801-806, 1988.
19) Kawakami, H.: Simulation of space-time variation of earthquake ground motion including a recorded time history. *Proc. JSCE*, No.410/I-12, pp.435-443, 1989 (in Japanese).
20) Kawakami, H.: Simulation of space-time variation of earthquake ground motion including time history of Imperial Valley earthquake. *Proc. 8th Japan Earthquake Engineering*, pp.1311-1316, 1990 (in Japanese).

21) Shinozuka, M, and Jan, C.-M.: Digital simulation of random processes and its applications, *Journal of Sound and Vibration*, Vol.25, No.1, pp.111-128, 1972.
22) Hoshiya, M.: Physical interpretation of simulation method of multi-dimensional random processes, *Proc. JSCE*, No.270, pp.131-134, 1978 (in Japanese).
23) Ishii, K.: Study on effects of input loss of earthquake waves by probabilistic method, *16th Japan Earthquake Engineering Symposium*, pp.317-320, 1981 (in Japanese).
24) Sawada, T.: Analysis of characteristics of earthquake motions and its applications, Doctoral thesis, Kyoto University, 1988 (in Japanese).
25) Katayama, T., Yamazaki, F., Nagata, S., Lu, L. and Turker, T. : Development of strong motion database for the Chiba seismometer array, Earthquake Disaster Mitigation Engineering, Institute of Industrial Science, University of Tokyo, January, 1990.
26) Hoshiya, M.: *Vibration Analysis using Probabilistic method*, Kashima Press, 1974 (in Japanese).
27) Hudson, D. *et al.*: Strong motion earthquake accelerograms, digitized and plotted data, *EERL* 71-50, California Institute of Technology, 1971.